A Phase Conjugator Based on Fourth-Order Subharmonically Pumped Mixers

Vinay **lyere**, Member, IEEE, Dustin Widmann, Graduate Student Member, IEEE, Christopher **Mooree**, Graduate Student Member, IEEE, Matthew F. Bauwens, Steven M. Bowerse, Senior Member, IEEE, and Robert M. Weiklee, Fellow, IEEE

Abstract-A new phase conjugator circuit architecture suitable for retrodirective array applications is described and demonstrated. The architecture is based on fourth-order subharmonically pumped mixers and requires a local oscillator (LO) frequency at half the radio frequency (RF). Measurements of a prototype phase conjugator operating at an RF input and intermediate frequency (IF) output of 3.47 and 3.57 GHz have shown an RF-to-IF conversion loss of 21.4 dB, RF-to-IF isolation of 26.4 dB, and isolation between the IF and twice the LO of 59.8 dB. A technique to quantitatively measure the phase conjugate signal that does not rely on retroreflection is also detailed.

Index Terms- Mixers, phase conjugator, retro-directive arrays, S-parameters, subharmonically pumped mixers.

I. INTRODUCTION

HASE conjugators, which are commonly used in retrodirective array applications [1], conventionally use mixers that produce output intermediate frequency (IF) signals at a frequency close to the input radio frequency (RF) signal. At microwave frequencies, it is common to realize phase conjugators using mixers with the local oscillator (LO) frequency at approximately double the RF. There are previous demonstrations in the literature that use an LO at twice the RF frequency such as [2], [3], and [4]. However, as operating frequencies increase, the requirement for significant power to pump the mix.er at twice the RF frequency can be expensive

Subharmonic mixers operate at a fraction of the RF and hence have advantages with regard to isolation between the LO and RF ports as well as available LO source power. For this reason, they are used extensively in the design and implementation of terahertz mixers as in [5] and [6]. Prior

Manuscript received 5 September 2023; revised 7 November 2023, 30 January 2024, and 13 March 2024; accepted 27 March 2024. This work was supported in part by the U.S. National Ground Intelligence Center (NGIC) "SMM Wave Device/System Development and Radar Signature Support" under Contract W91IW5-16-C-0007 and Contract W50NH9-21-C-00013, and in part by the NSF SPECEES Program and through a subcontract to NSF (SpectrumX- An NSF Spectrum Innovation Center) under Grant AST-2132700. (Corresponding author: Vinay lyer.)

Vinay Iyer is with Nokia of America Corporation, Sunnyvale, CA 94085 USA (e-mail: vvi4hc@virginia.edu).

Dustin Widmann, Christopher Moore, and Steven M. Bowers are with the Department of Electrical and Computer Engineering, University of Virginia, Charlottesville, VA 22903 USA.

Matthew F. Bauwens is with Dominion MicroProbes, Inc., Charlottesville, VA 22903 USA.

Robert M. Weikle is with the Department of Electrical and Computer Engineering, and the Department of Physics, University of Virginia, Charlottesville, VA 22903 USA.

Color versions of one or more figures in this letter are available at https://doi.org/10.1109/LMWT.2024.3383333.

Digital Object Identifier IO.1109/LMWT.2024.3383333

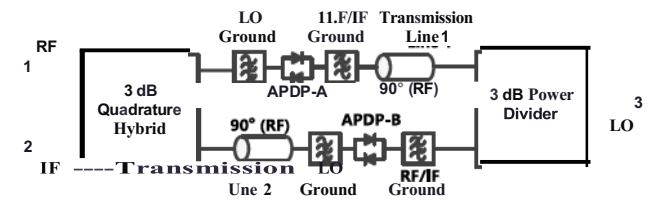


Fig. I. Circuit architecture of the phase conjugator based on fourth-order subharmonically pumped mixers. The transmission lines I and 2 are 90° at the RF frequency. The RF, IF, and LO ports are indicated.

work [7] described the use of a phased LO to obtain a high order of mixing. Subharmonic mixers also find use in phase conjugation circuits. A phase conjugator technique that used an LO at the same frequency as the RF was detailed in [8]. Frequency separation can be an issue in such designs if not accounted for appropriately. An array that operated with LO at a fourth of the RF frequency was published in [9]. An array with the LO at one-half the frequency of the RF like this work was detailed in [10] and [11], but these are integrated with antennas and do not have an intrinsic separation between the RF and IF port like our work does. More recent demonstrations include all-optical frequency dissemination using photonic microwave phase conjugation [12], and an active retrodirective antenna technique for circularly polarized wireless power transmission as in [13].

In this work, a phase conjugator architecture based on fourth-order subharmonically pumped mixers using an LO with frequency at approximately half the RF is described. Analysis and design of the circuit are discussed, and a prototype version operating close to 1.7 GHz is demonstrated. This work also details a technique to quantitatively measure the phase conjugate signal at the RF frequency at the IF port, in the presence of leak.age from the RF and LO ports, unlike previous work that relies on retroreflection measurements.

II. CIRCUIT ANALYSIS AND DESIGN

Fig. 1 shows the basic circuit topology of the phase conjugator. Two antiparallel diode pairs (APDPs) are employed for subharmonic mixing. The LO signal (wp WRJi/2) is divided and applied to drive the APDPs with equal amplitudes and 45° phase offset (corresponding to the electrical length of transmission line 1 at the LO frequency). The RF signal is fed to the APDPs using a 3-dB quadrature hybrid with a 90° delay line (transmission line 2) connecting the hybrid's quadrature port to APDP-B. This provides two equal-amplitude RF signals to the APDPs with a 180° phase offset

It is well established that the sideband currents present at the terminals of the APDPs can be expressed in terms of the small-signal sideband voltages, Vn, and a conversion admittance matrix [14), [15]. The elements of the conversion admittance

matrix, Ym,n, are functions of the Fourier components of the conductance (Gk) and capacitance (Ck) waveforms of the pumped diodes

$$Y_{m,n} = G_{m-n} + j(\omega_0 + m\omega_p)C_{m-n} \tag{I}$$

where Wo and wp are the IF and LO frequencies, respectively. The LO phase offset applied to APDP-A through delay line I results in a Linear (with frequency) phase shift of each Fourier component of the diode pair's conductance and capacitance waveforms [5]. Thus, the sideband currents flowing through APDP-A and APDP-B can be expressed as

$$I_{m} = Y_{m,n} \exp \frac{4}{2} V_{n}$$
 (2)

and

$$/mB = \prod_{n=-00}^{00} Y_{m,n} V_n.$$
 (3)

In (2) and (3), superscripts A and B refer to the specific APDP, m is the current sideband index, n is the voltage sideband index, and Y_m is the *mnth* element of the conversion admittance matrix. Consistent with the literature, the angular frequency corresponding to sideband n is defined as $\{q\}+nwp$. Thus, a sideband index of m = 0 corresponds to the IF current The negative sign in (3) arises from the 180° phase difference between the RF signals at the output of the hybrid. Examination of (2) and (3) readily shows that the IF currents at the terminals of the APDPs that are associated with the input RF signal (at sideband n = -4, corresponding to WRF::::: 2wp) are in phase. As a result, the IF signals (whkh are at approximately the same frequency as the RF input signal) cancel at the RF input (port 1) of the quadrature hybrid and sum at the IF output (port 4). Conversely, the RF currents (with sideband indices of m = -4) are 180° out of phase, resulting in cancellation at the IF output (port 4). In addition, because the RF input is applied and the IF output is taken at mutually isolated ports of the hybrid, coupling between the input RF and its phase-conjugate rep]jca at the IF output is minimized. Isolation between these signals is examined further through measurements on a prototype phase-conjugator based on the architecture of Fig. I.

Ill. IMPLEMENTATION

A prototype phase conjugator based on the archHecture of Fig. I has been implemented as a microstrip circuit fabricated on an FR4 4-layer substrate (with a dielectric constant of 3.61, a substrate thickness of approximately 55 mils, and a top conductor thickness of approximately 1.7 mils). The PCB is 64.5-mm Jong and 45.8-mm wide. The transmission lines and circuit components are designed with the ground being on the second metal layer. The circuit is designed to operate at an RF of 3.47 GHz, an LO frequency of 1.76 GHz, and an IF of 3.57 GHz. The circuit layout is shown in Fig. 2 and consists of a branchline coupler as the 3-dB quadrature hybrid and a meandered WiWnson coupler as the LO power divider. Two pairs of GaAs Schottky antiparallel diode pairs (Model MA4El318 from Macom) are flip-chip soldered onto the circuit. Electrical parameters (obtained from the datasheet) for these devices are provided in Table I.

In addition to the two delay lines required for proper phasing of the RF and LO signals, several microstrip Lines and stubs designed using the harmonic balance simulator of Keysight's

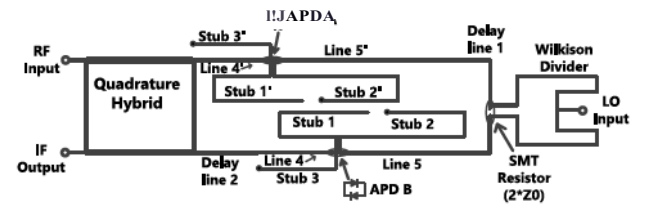


Fig. 2. Microstrip layout of the fourth-order subharmonic phase conjugator.

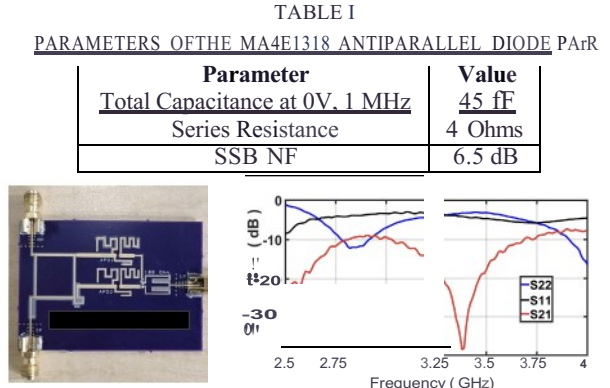


Fig. 3. (a) Photograph of the PCB. (b) Measured S-parameters of the phase conjugator. RF input is at port I [on top in (a)], and IF output is at port 2 [on bottom in (a)].

Advanced Design System software are included as idlers and impedance matching networks. Stubs 3 and 3' (90° at the RF) are used as idlers for mixing products at the frequencies WRF + 2wp = 6.99 GHz, -(WRF- 2wp) = 50 **MHz**, and WRF+ 6wp = 14.03 GHz. ANSYS high-frequency simulation software (HFSS) is used to simulate the complete layout. Fig. 3(a) shows an image of the prototype.

IV. MEASUREMENTS

A S-Parameter and Large-Signal Measurements

The RF/IF matching and isolation of the phase conjugator were measured using a Keysight PNA vector network analyzer. During this measurement, a 1.7-GHz source with an avajJable power of 10.1 dBm was applied to the LO port of the circuit The measured S-parameters are shown in Fig. 3(b), where S11, S22, and S21 represent the RF input matching, IF output matching, and RF-to-IF isolation, respectively. Measurements of RF-to-IF conversion loss and 2 LO-to-IF isolation (ratio of the available LO power to the LO second-harmonic power at the IF port) were done using swept-frequency sources applied to the LO and RF ports with a spectrum analyzer at the IF port. The LO, RF, and IF are fixed at 1.693, 3.41, and 3.362 GHz (from a sweep for optimal performance), respectively, with an available LO power of 10.1 dBm. The simulated and measured performance of the prototype phase conjugator at the given frequencies are summarized in Table II.

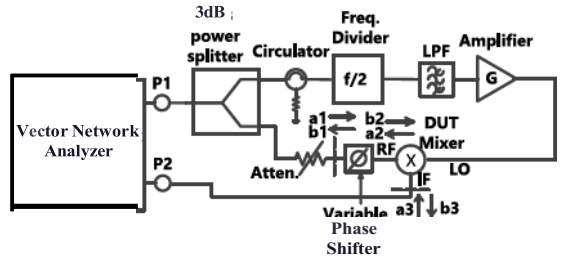
A prior prototype based on the architecture of Fig. 2 implemented as a microstrip circuit, fabricated on a Roger's RT/duroid 5880 substrates at an RF of 2 GHz had conversion loss of 13 dB, and RF-to-IF isolation of 38 dB. The high conversion loss and the disparity between simulated and measured return loss in this prototype are attributed to the use of an FR4 substrate at a higher frequency and imprecise diode models.

B. Phase Conjugation Measurement

A technique to quantify the phase conjugate signal using S-parameters is devised as shown in Fig. 4. The signal

TABLE II MEASURED AND SIMULATED PERFORMANCE OF THE PHASE CONJUGATOR

Parameter	Simulated	Measurement
Conversion Loss(dB)	26	21.4
RF to lF isolation (dB)	29	26.5
2 LO to IF isolation (dB)	Inf	59.8
Avail. LO power (dBm)	13.5	IO.I



Metrology scheme for demonstrating phase conjugation using the DUT mixer and a COTS frequency divider with reference planes indicated.

from Port 1 is divided using a 3-dB power splitter, and one of the ports is connected to a circulator followed by a prescaler (Pasternack PE88D2001) to divide the frequency by 2, a low-pass filter (Minicircuits VLP-16), and an amplifier (Minicircuits ZVE-8G+) in that sequence. This signal supplies the LO to the OUT mixer examined above. Next, the signal from the second port of the 3-dB splitter is supplied to an attenuator followed by a phase shifter. The phase shifter is a delay line that operates over the band of the RF signal. This signal is connected to the RF port of the OUT mixer. The IF port is connected to Port 2 of the VNA. The reference planes for the two-port S-parameter calibration are shown in the scheme as well. The phase shifter enables the introduction of a phase shift in the RF path relative to the LO path. Consider the various complex wave amplitudes as detailed in Fig. 4. a, $\sqrt{3}$, y, and E are complex constants that characterize the response of the circuit to the RF and LO signals

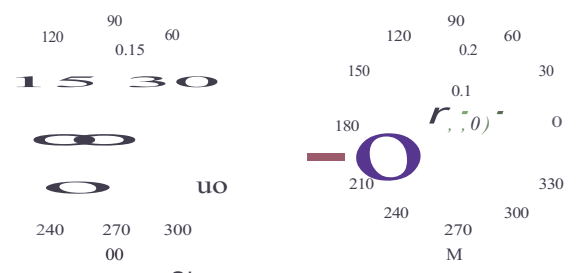
$$b2 = a, eU (>)$$
 (4)

$$b3 = ab2 + f3b2 + y = w,eU(\phi) + 8a,e<-j(\phi) + y$$
 (5)

$$S_{21} = b_3/a_1 = \epsilon e^{(j\phi)} + \nu e^{(-j\phi)} + \mu \tag{6}$$

where E, v, and μ , are complex constants that indicate the quantities of the RF leakage, phase conjugate signal, and LO leakage all normalized to the input RF wave, respectively. This contour sketches out an ellipse in the </> plane. The eccentricity and the foci are dictated by the terms in (6). The LO leakage drives the offset from the origin of the contour, and the strength of the phase conjugate signal versus the RF leakage drives the direction the contour is traced out in. For equal parts RF leakage and phase conjugate signal, the contour is a line. To prove the validity of the theory, a large-signal S parameter simulation (LSSP) is performed in ADS, with the RFand IF ports excited at 3.5 GHz and the LO port excited at 1.75 GHz. As expected, the contour traced is an ellipse as shown in Fig. 5(a). The contour is also centered at the origin consistent with infinitesimally small 2*LO to IF leakage (Table II). Next, the LSSP simulation of the prototype is adapted to introduce a finite LO leakage and S_{21} is plotted. This is shown in blue in Fig. 5(b).

To characterize the behavior of the phase shifter, a two-port S-parameter measurement is performed as the phase sett.ing is altered. The phase shifter has uniform insertion loss (near 0 dB) over the delay settings. Next, the VNA (used in the CW mode) is calibrated at 3.455 GHz at the reference planes indicated in the scheme with the amplifier and the frequency divider biased at quiescent. These two ports are then connected Jeffrey Hesler, Virginia Diodes Inc., for technical discussions.



(a) Simulated Si of the prototype across phase shift settings. (b) Measured (brown scatter plot). fit (red contour). and simulated (blue contour) S21 of the OUT mixer with the LO path on. Measured S21 of the prototype with LO off is shown in green. The black arrows indicate the direction traced on the contours with increasing delay setting.

TABLE ill COMPLEX PARAMETERS FROM ELLIPSE CURVE-FITTING

Coefficie	nt	Complex value	Mag. (linear)	dB norm.
I;		-0.01345+0.01565i	0.0206	-9.0
//		O.D3 + 0.0553i	0.0629	-4.2
μ		-0.1555 - 0.05506i	0.1650	0

as shown in the scheme and S₂₁ measured with first the divider and amplifier being turned off, and then with both on. Fig. 5(b) plots these two cases with the arrow indicating the contour direction as delay increases. With LO off, a clockwise contour is traced. With the LO on, the points now trace an ellipse offset from the center in the counterclockwise direction, as expected since the phase conjugate signal dominates.

The contour shown in Fig. 5(b) (in red) is fit to (6) to quantify the various components. This is shown in Fig. 5(b) in blue. The quantities E, μ_{ij} , and ν are listed in Table III. The values in the fourth column are normalized to the value of the LO leakage. As can be interpreted based on the contour and confirmed by the analysis, the LO leakage dominates. The phase conjugate term is stronger than the RF leakage as expected, as well. The root mean squared error (RMSE) of the fit is 0.008. The normalized powers correlate exceedingly well with the large signal measurements in Table II (5 dB difference between the RF leakage and the conversion loss to phase conjugate signal). The leakage from RF (attributable to only the phase conjugator) is expected to be much lower in future work, specifically with rigorous modeling of the diodes and the use of a substrate appropriate at the frequencies being measured. The instrument dynamic range and setup do introduce artifacts that cause deviations from the ideal elliptical behavior as is seen in our measurements. In cases where the measurement setup is a limiting factor, the combination of the large-signal measurements and the phase conjugation measurements (and agreement between the two as shown in Table III) can be used to corroborate results.

V. CONCLUSION

A phase conjugator architecture suitable for extension to mm-wave bands is demonstrated at RF frequencies on a lowfrequency prototype PCB. The circuit uses a fourth harmonic mixer relaxing the frequency requirement on the LO considerably. In addition, a metrology technique to characterize the actual degree of phase conjugation without relying on frequency separation is illustrated and demonstrated.

ACKNOWLEDGMENT

The authors thank N. Scott Barker and Travis N. Blalock, University of Virginia, Zhiyang Liu, Skyworks Inc., and

REFERENCES

- [I] R. Y. Miyamoto and T. Itoh, "Retrodirective arrays for wireless communications," *IEEE Mierow. Mag.*, vol. 3, no. I, pp. 71-79, Mar. 2002, doi: IO.I109/6668.990692.
- [2] C. W. Pobanz and T. Itoh, "A conformal retrodirective array for radar applications using a heterodyne phased scattering element," in *IEEE M1T-S Im. Mierow. Symp. Dig.*, vol. 2, Orlando, FL, USA, May 1995, pp. 905-908, doi: 10.1109/MWSYM.1995.405902.
- [3] K. M. K. H. Leong, R. Y. Miyamoto, and T. Itoh, "Moving forward in retrodirective antenna arrays," *IEEE Potentials*, vol. 22, no. 3, pp. 1–21, Aug. 2003, doi: I0.1109/MP.2003.1232308.
- [4] K. M. K. H. Leong, Y. Wang, and T. Itoh, "A full duplex capable retrodirective array system for high-speed beam tracking and pointing applications," *IEEE Trans. Mierow. Theory Techn.*, vol. 52, no. 5, pp. 1479-1489, May 2004, doi: 10.1109/TMTT.2004.827025.
- [5] W. L. Chang and C. Meng, "A miniature 200-GHz subharmonic mixer with a folded 1800 hybrid using equal-length edge- and broadsidecoupled lines," *IEEE Mierow. Wireless Compon. Lett.*, vol. 28, no. 4, pp. 338-340, Apr. 2018, doi: 10.1109/LMWC.2018.2811252.
- [6] Y. Liu, B. Zhang. Z. Niu. Y. Feng, and Y. Fan, "A novel 180-210 GHz single sideband mixer using filtering waveguide-microstrip transition structure," *IEEE Microw. Wireless Technol. Lett.*, vol. 33, no. 6, pp. 727-730, Jun. 2023, doi: 10.1109/LMWT.2023.3248061.
- [7] Z. Liu and R. M. Weikle, "High-order subharmonically pumped mixers using phased local oscillators," *IEEE Trans. Mierow. The*ory Teclm., vol. 54, no. 7, pp. 2977-2982, Jul. 2006, doi: 10.1109/TMTT.2006.876986.
- [8] T. Brabetz, V. F. Fusco, and S. Karode, "Balanced subharmonic mixers for retrodirective-array applications," *IEEE Trans. Mierow. Theory Techn.*, vol. 49, no. 3, pp. 465-469, Mar. 2001, doi: 10.1109/22.910549.
- [9] 1.-Y. Park and T. Itoh, "A 60-GHz 4th subharmonic phase-conjugated retrodirective array," in *Proc. 34th Eur. Mierow. Conf.*, Amsterdam, Netherlands, Oct. 2004, pp. 1277-1280.
- [JO] B. T. Murakami, J. D. Roque, S. S. Sung, G. S. Shiroma, R. Y. Miyamoto, and W. A. Shiroma, "A quadruple subharmonic phaseconjugating array for secure picosatellite crosslinks," in *IEEE M1T-S Int. Mierow. Symp. Dig.*, Fort Worth, TX, USA, Jun. 2004, pp. 1687-1690, doi: 10.1109/MWSYM.2004.I338914.
- [II] J.-Y. Park, K. M. K. H. Leong, T. Itoh. G.-R. Kim, and J.-I. Choi, "Planar active retrodirective array with subharmonic phase conjugation mixers," in *Proc. Asia-Pacific Mierow. Conj*, vol. I, 2003, pp. 170-173.
- [12] D. N. Held and A. R. Kerr, "Conversion loss and noise of microwave and millimeterwave mixers: Part 2--Experiment," *IEEE Trans. Mierow. Theory Teehn.*, vol. MTT-26, no. 2, pp. 55-61, Feb. 1978, doi: 10.1109/TMTT.1978.1129313.

- [13] A. R. Kerr, "Noise and loss in balanced and subharmonically pumped mixers: Part I-Theory," *IEEE Trans. Mierow. Theory Teehn.*, vol. MTT-27, no. 12, pp. 938-943, Dec. 1979,doi: 10.1109/TMTT.1979. I129771.
- [14] H. Wang, X. Xue, S. Li, and X. Zheng, "All-optical arbitrary-point stable quadruple frequency dissemination with photonic microwave phase conjugation," *IEEE Photon. J.*, vol. 10, no. 4, pp. 1-8, Aug. 2018, doi: 10.1109/JPHOT.2018.2856515.
- [15] P. D. H. Re, S. K. Podilchak, C. Constantinides, G. Goussetis, and J. Lee, "An active retrodirective antenna element for circularly polarized wireless power transmission," in *Proc. IEEE Wireless Power Transf Conj (WPTC)*, Aveiro, Portugal, May 2016, pp. 1-4, doi: 10.1109/WPT.2016.7498805.
- [16] D. N. Held and A. R. Kerr, "Conversion loss and noise of microwave and millimeterwave mixers: Part I-Theory," *IEEE Trans. Microw. Theory Teclm.*, vol. MTT-26, no. 2, pp. 49-55, Feb. 1978, doi: 10.1109/TMTT.1978.1129312.
- [17] A. R. Kerr, "Noise and loss in balanced and subharmonically pumped mixers: Part II-Application," *IEEE Trans. Mierow. The*ory Teclm., vol. MTT-27, no. 12, pp. 944-950, Dec. 1979, doi: 10.1109/TMTT.1979.1129772.
- [18] H. Xu, Y. Duan, J. L Hesler, T. W. Crowe, and R. W. Weikle, "Subharmonically pumped millimeter-wave upconverters based on heterostructure barrier varactors," *IEEE Trans. Mierow. Theory Techn.*, vol. 54, no. 10, pp. 3648-3653, Oct. 2006, doi: 10.1109/TMTT.2006. 882890.
- [19] A. R. Kerr, "Noise and conversion loss analysis of two-diode subharmonically pumped and balanced mixers," in *IEEE M1T-S Int. Mierow. Symp. Dig.*. Orlando, FL, USA, Apr. 1979. pp. 17-18, doi: 10.1109/MWSYM.1979.1123955.
- [20] A. R. Kerr, "A technique for determining the local oscillator waveforms in a microwave mixer (short papers)," *IEEE Trans. Microw. Theory Techn.*, vol. MTT-23, no. JO. pp. 828-831, Oct. 1975, doi: 10.1109/TMTT.1975.1128691.
- [21] C. A. Allen, K. M. K. H. Leong, and T. Itoh, "A negative reflective/refractive 'meta-interface' using a bi-directional phase-conjugating array," in *IEEE MTT-S Im. Mierow. Symp. Dig.*, Philadelphia. PA, USA, Jun. 2003, pp. 1875-1878, doi: 10.1109/MWSYM.2003. 1210522
- [22] L. D. Didomenico and G. M. Rebeiz, "Digital communications using self-phased arrays," *IEEE Trans. Mierow. Theory Techn.*, vol. 49, no. 4, pp. 677-684, Apr. 2001, doi: 10.1109/22.915442.
- [23] V. Fusco and N. B. Buchanan, "High-performance IQ modulator-based phase conjugator for modular retrodirective antenna array implementation," *IEEE Trans. Mierow. Theory Techn.*, vol. 57, no. 10, pp. 2301-2306, Oct. 2009, doi: 10.1109/TMTT.2009.2029033.